PLY-BY-PLY BASIS OFF-AXIS FATIGUE LIFE PREDICTION FOR CROSS-PLY CFRP LAMINATES AT ROOM TEMPERATURE

Masamichi KAWAI* and Naruhiko HONDA**
*** Department of Engineering Mechanics and Energy, University of Tsukuba**
**** Graduate School of Systems and Information Engineering, University of Tsukuba**

Keywords: *cross-ply laminate, off-axis fatigue, S-N relationship, ply-by-ply basis analysis, ply fatigue model, in-situ strengths, plastic deformation*

Abstract

Off-axis fatigue behavior of a symmetric cross-ply carbon/epoxy laminate is examined at room temperature and a fatigue life prediction method that considers inelastic deformation and in-situ strength of embedded plies is developed. The fiber orientation dependence of the off-axis fatigue data on the cross-ply laminate can be removed by normalizing them with respect to static strength. The distribution of the normalized off-axis fatigue data of the cross-ply laminate almost agrees with the result for the unidirectional laminates made of the same prepreg tape. Then, off-axis fatigue analysis of cross-ply laminates is performed on a ply-by-ply basis. For this purpose, a ply fatigue model that takes into account in-situ static strengths of plies embedded in a laminate is proposed. Stresses in the cross-ply laminate are evaluated using a CLT-based laminate constitutive model that considers nonlinear deformation of embedded plies. Predicted off-axis fatigue lives of the cross-ply laminate are shown to correlate well with experimental results.

1. Introduction

In developing a fatigue model applicable to plies embedded in multidirectional laminates, in-situ static and fatigue strengths of plies should appropriately be taken into account. Constraint of ply strain in a laminate results in higher ply strength compared with the ply strength in a unidirectional laminate. The in-situ effect on ply strength depends on degree of interaction between adjacent plies. This explains that strength of a laminated composite is largely dependent on thickness of laminate, number of adjacent plies with the same orientation and stacking sequence of plies with different orientation. Quantification of in-situ effects are attempted in the studies [1-5].

Although ply-by-ply basis prediction of S-N relationship of laminates has been attempted so far, for example, by Rotem-Hashin [6], Rotem [7], Lee et al. [8], Gao [9], very few studies address in-situ strength based prediction of fatigue life of multidirectional laminates, which is partly because only a limited amount of information is available on the in-situ fatigue strength of plies in a laminate in contrast to a tolerable amount of information on in-situ static strength. Recently, Kawai and Maki [10] discussed a ply-by-ply basis fatigue life prediction method for a symmetric alternating cross-ply carbon/epoxy laminate subjected to cyclic loading in the fiber direction. On the basis of two observations that 1) the accurate prediction of the tensile strength of the cross-ply laminate required consideration of the in-situ strength of embedded plies and 2) the in-situ fatigue behavior of embedded plies was insensitive to the number of plies, they developed a ply fatigue model by replacing the principal static strengths used in the fatigue model for unidirectional composites [11] with in-situ principal static strengths. A simple laminate fatigue model based on the ply fatigue model and the assumption that fatigue strength of a laminate is determined by failure of main load bearing plies has succeeded in adequately predicting the S-N relationship of the cross-ply laminate.

In the present study, in-situ strength based fatigue life prediction for a symmetric alternating cross-ply carbon/epoxy laminate subjected to off-axis fatigue loading is attempted on a ply-by-ply basis. First, tension-tension fatigue tests are carried out at room temperature for three kinds of off-axis fiber orientations to examine the off-axis S-N

relationship and its fiber orientation dependence of the cross-ply laminate. A laminate fatigue model is formulated by integrating the ply fatigue model into the classical laminate theory. Nonlinear deformation of embedded plies under off-axis loading is taken into account for accurately evaluating the stresses in the embedded plies. Finally, validity of the proposed laminate fatigue model is evaluated by comparing with experimental results.

2. Materials and Testing Procedure

2.1 Material and specimens

Symmetrical alternating cross-ply CFRP laminates with a $[0/90]_{3S}$ lay-up were manufactured by the autoclave forming technique. The curing temperature was 130°C. The prepreg tape T800H/2500 (P2053-17, TORAY) made of carbon fiber T800H and thermosetting epoxy resin #2500 was used. The prepregs were laid up by hand and autoclaved.

Five kinds of plain coupon specimens with different fiber orientations $[\theta/(90\text{-}\theta)]_{3S}$ (θ = 0, 5, 15, 45, 90°) were cut from a 400 by 400 mm cross-ply laminate panel to dimensions of the specimen length L = 200 mm, the width W = 20 mm and the thickness t = 2.25 mm, following the testing standards JIS K7073 and JIS K 7083. Rectangular-shaped tabs of 1.0 mm thick aluminum alloy were glued on both ends of the specimens with epoxy adhesive (Araldite).

2.2 Testing procedure

On- and off-axis fatigue tests were performed at room temperature (RT, ~23°C) under load control. Fatigue load was applied in a sinusoidal waveform with a frequency of 10Hz and a stress ratio of R = 0.1 ($R = \sigma_{min}/\sigma_{max}$), following the testing standards: JIS K 7083 and ASTM D3479. The specimens were fatigue tested for up to 10^6 cycles. Maximum fatigue stresses were determined so as to obtain fatigue data within the life range from 10^3 to 10^6 cycles. Prior to fatigue testing, static tension tests were performed at room temperature to identify the off-axis ultimate tensile strengths of the cross-ply laminate, following the testing standards JIS K7073 and ASTM D3039.

The static and fatigue test were conducted in a servo-hydraulic testing machine. The longitudinal and lateral strains of specimens were monitored with two-elements rosette strain gauges. No attempt was made to control the moisture content of the specimens.

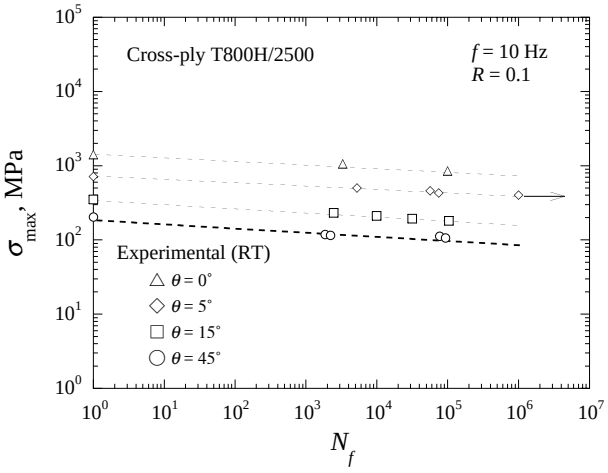

Fig. 1 S-N relationships σ_{max} - N_f for all fiber orientations at room temperature (f = 10 Hz, R = 0.1)

3. Experimental Results and Discussion

The in-plane specimen coordinate system is denoted as (x, y) and the x-axis is taken to be in the longitudinal direction of coupon specimens. The principal axes of material anisotropy for individual plies are expressed as (1, 2) with the 1-axis being in the fiber direction. The fatigue load is given in the x-axis direction.

3.2 Constant-amplitude off-axis fatigue behavior

3.2.1 Off-axis S-N relationships

The S-N relationships of the cross-ply laminate at RT are shown in Fig. 1 for all the fiber orientations, as a plot of the maximum fatigue stress σ_{max} against the number of cycles to failure N_f on logarithmic scales. The static tensile strength data are plotted at $N_f = 10^0$ as points of the ordinate in the S-N diagram.

Regardless of the fiber orientation, the log-log plots of the fatigue data can approximately be described using a straight line with a negative slope over the range of fatigue life up to 10^6 cycles. The dashed straight lines fitted to the fatigue data for respective fiber orientations are almost parallel with each other, and they are approximately extrapolated back to the points indicating the static tensile strengths. The fatigue endurance limits were not observed in the range of fatigue life up to 10^6 cycles. This observation suggests that the power-law approximation of the Basquin type with an identical value of fatigue exponent can be used for describing the S-N relationships in a consistent manner within

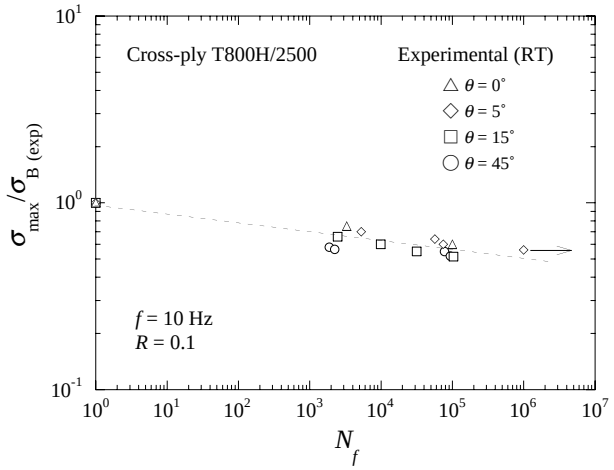

Fig. 2 Normalized S-N relationships at RT using experimental fatigue strength ratio

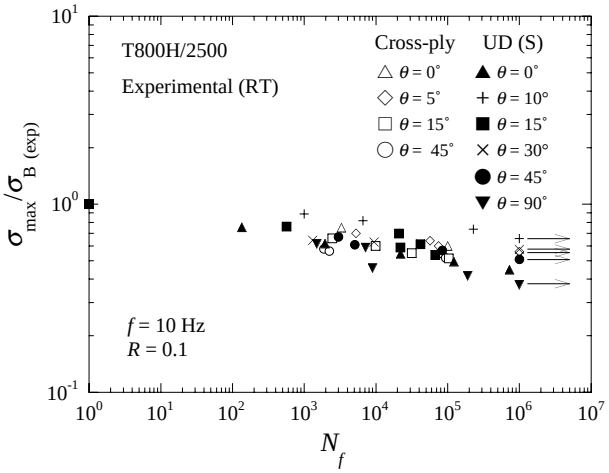

Fig. 3 Comparison of the normalized S-N relationships for unidirectional and cross-ply laminates at room temperature using experimental fatigue strength ratio

the accuracy involved by the log-log scale for all the fiber orientations. The straight-line approximation of the S-N data also indicates that the fatigue strength for a fatigue life of $N_f = 10^6$ reduces to as low as 86% of the tensile strength, regardless of the fiber orientation.

3.2.2 Normalized S-N relationships

Effects of difference in fiber orientation on the fatigue behavior of the cross-ply laminate can be observed by comparing the normalized fatigue strengths. Fig. 2 shows comparison between the normalized S-N relationships using the normalized stress level $\sigma_{\max} / \sigma_{B(\exp)}$ ($\sigma_{B(\exp)}$: the observed static tensile strength). The normalized fatigue data of the cross-ply laminate are distributed in a narrow band regardless of the fiber orientation, and they are approximately fitted to a single straight line over the range of fatigue life. This indicates that the fiber orientation dependence of the off-axis S-N relationship of the cross-ply laminate can approximately be removed using the experimental strength ratio.

The off-axis fatigue behavior of the cross-ply laminate $[0/90]_{3S}$ is compared with that the unidirectional laminate $[0]_{12}$ [13]. Fig. 3 shows the plots of the normalized stress level against the number of cycles to failure for the two kinds of laminates at RT. The normalized S-N relationships for the cross-ply and unidirectional laminates almost agree with each other. This indicates that the maximum fatigue stress dependence of fatigue behavior for the cross-ply laminate is substantially identical with that for the unidirectional laminate. It is important to note that the difference between the fatigue behaviors of those laminates can be eliminated by the normalization of fatigue data by means of the static strengths. Consequently, a good agreement between the normalized S-N relationships for those laminates implies that the off-axis fatigue strength of the cross-ply laminate is determined by the off-axis fatigue strength of the constituent axial plies.

3.2.3 Fatigue failure morphology

Macroscopic fatigue failure morphology for θ = 0, 15, 45° is shown in Fig. 4. The fatigue failure of 0° specimens occurred with pullout of fiber bundle and extensive delamination which were less significant in the case of static tensile fracture. For the other fiber orientations $0° < \theta \leq 90°$, the coupon specimens failed in through-thickness cross-sections along fibers with extensive delamination, which is similar to the static failure morphology. In the case of fatigue failure, delamination was more extensive and pullout of fibers was more remarkable compared with the case of static tensile failure. For the specimens survived at the number of cycles 10^6 cycles, delamination and matrix cracks were also observed, but they were not so remarkable as in the specimens failed completely in fatigue.

4. A Ply-By-Ply Basis Fatigue Life Analysis

It was confirmed that the off-axis fatigue behavior of the cross-ply laminate was similar to

(a) $\theta = 0°$

(b) $\theta = 15°$

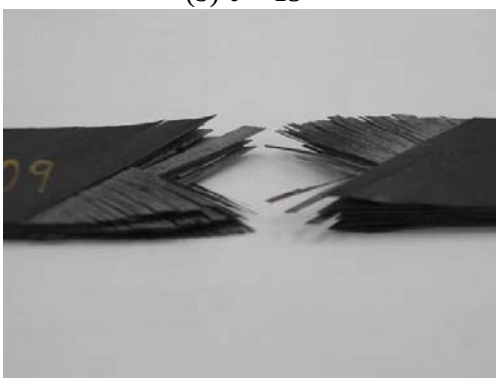

(c) $\theta = 45°$

Fig. 4 Specimens failed in fatigue at room temperature

that of the unidirectional laminate made of the same type of prepreg tape. In present study, a fatigue life prediction method is proposed for alternating cross-ply laminates by assuming that the relative fatigue performance of constituent unidirectional plies agrees with that of isolated thick unidirectional laminates for any fatigue loading conditions, with the exception of their principal strengths which are changed by in-situ effects.

4.1 Non-dimensional effective stress

In the previous study [12], it was confirmed that a fatigue strength ratio becomes an effective parameter to cope with the off-axis fatigue behavior of unidirectional laminates. Furthermore, as a generalized parameter of the empirical strength ratio, a non-dimensional effective stress was defined on the basis of the Tsai-Hill static failure criterion for orthotropic media and used to formulate a fatigue damage mechanics model for the off-axis fatigue behavior of unidirectional laminates.

In the present study, we attempt to apply the phenomenological fatigue model originally developed for unidirectional laminates to unidirectional plies embedded in the cross-ply laminate. For this purpose, the non-dimensional effective stress is generalized to take into account an in-situ effect on the strengths of plies. For the case of plane stress, a modified form of the non-dimensional effective stress is expressed as [6]

$$\sigma^* = \sqrt{\left(\frac{\sigma_{11}}{X^*}\right)^2 - \frac{\sigma_{11}\sigma_{22}}{X^{*2}} + \left(\frac{\sigma_{22}}{Y^*}\right)^2 + \left(\frac{\tau_{12}}{S^*}\right)^2} \qquad (1)$$

in the fiber coordinate system, where X^* and Y^* represent the longitudinal and transverse in-situ strengths and S^* denotes the in-situ shear strength along the fiber direction.

From a practical point of view, it may be convenient for those in-situ strengths to be designated as

$$X^* = \alpha X \qquad (2)$$

$$Y^* = \beta Y \qquad (3)$$

$$S^* = \gamma S \qquad (4)$$

where X, Y, S stand for the reference principal strengths of a comparison unidirectional composite. The scaling factors α, β, γ represent the in-situ strength ratios, and they depend on the degree of strain constraint of plies in laminates [6]. In general contexts, therefore, the in-situ strength ratios should be treated as functions of the thickness of plies as well as the orientation of adjacent plies, although they are fixed at particular values in the present study.

4.2 A ply fatigue model

For description of a brittle-natured damage growth in unidirectional plies, the following form of evolution equation is used [6, 11, 12]:

$$\frac{d\omega}{dN} = K{\sigma^*_{\max}}^n \left(\frac{1}{1-\omega}\right)^k \tag{5}$$

where ω is a measure of damage, $\sigma^*_{\max}$ is the maximum non-dimensional effective stress associated with the maximum fatigue stress, and K, n and k are material constants.

Impose the initial condition that $\omega = 0$ when $N = 0$ and assume that the final fracture occurs at the instant when ω reaches unity. Then, integrating Eq. (5) under a constant stress cycling condition, we can obtain an analytical expression of fatigue life as

$$N_f = \frac{1}{(k+1)K\left(\sigma^*_{\max}\right)^n} \tag{6}$$

Setting $N_f = 1$ when $\sigma^*_{\max} = 1$, we find $(k+1)K = 1$. This yields the fatigue life equation of the following form:

$$N_f = \frac{1}{{\sigma^*_{\max}}^n} \tag{7}$$

This relation indicates that a linear master S-N relationship is obtained for a given stress ratio by plotting the fatigue strength parameter $\sigma^*_{\max}$ against the number of cycles to failure N_f on logarithmic scales.

4.3 A laminate fatigue model

To calculate the fatigue life of plies embedded in the cross-ply laminates using the fatigue life equation described above, it is required to calculate the state of stress in those plies. In the case of alternating cross-ply laminate considered in this study, once the stress components in the θ and (90-θ) plies are evaluated for a given maximum fatigue stress $\sigma_{\max}$ loaded in the longitudinal direction (x-axis direction), we can calculate the maximum non-dimensional effective stresses ${}^{\theta}\sigma^*_{\max}$, ${}^{90-\theta}\sigma^*_{\max}$ in the θ and 90-θ plies.

For a ply-by-ply basis fatigue analysis, it is assumed that fatigue failure of cross-ply laminate is substantially determined by fatigue failure of critical plies that have a larger safety margin to static failure left for a given external load due to their more sustainable orientation of fibers. For the fatigue loading conditions dealt with in this study, the safety margin to static failure for a given maximum fatigue load, $1-\sigma^*_{\max}$, turns to be larger in the θ plies, and thus the θ plies become critical plies in the alternating cross-ply laminate. Under the present assumption, therefore, the off-axis fatigue life of the symmetric alternating cross-ply laminate can be calculated using the following formula:

$${}^{CP}N_f \simeq {}^{\theta}N_f \tag{8}$$

4.4 A laminate constitutive model

Off-axis tensile behavior of cross-ply laminate is analyzed using the classical laminate theory and plastic model of ply. The state of stress of plies in the cross-ply laminate associated with an off-axis maximum fatigue load is calculated by applying the Sun-Chen plasticity model [13] to the nonlinear behavior of individual plies with the classical laminated plate theory.

The Sun-Chen model is a plasticity model for orthotropic composites, and it is assumed that no plastic strain occurs in the fiber direction of plies. The Sun-Chen model has been reduced to a useful form for plane stress condition, and it is expressed as

$$d\boldsymbol{\varepsilon}^p = \frac{3}{2}\frac{\overline{d\varepsilon^p}}{\bar{\sigma}}\mathbf{B}\boldsymbol{\sigma} \tag{9}$$

where

$$d\boldsymbol{\varepsilon}^p = \{d\varepsilon^p_{11}, d\varepsilon^p_{22}, d\gamma^p_{12}\}^T \tag{10}$$

$$\boldsymbol{\sigma} = \{\sigma_{11}, \sigma_{22}, \tau_{12}\}^T \tag{11}$$

stand for the plastic strain increment and stress vectors, respectively, and $\bar{\sigma}$, $\overline{d\varepsilon^p}$ are the equivalent stress and the equivalent plastic strain increment which are respectively defined as

$$\bar{\sigma} = \sqrt{\frac{3}{2}\boldsymbol{\sigma}^T\mathbf{B}\boldsymbol{\sigma}} \tag{12}$$

$$\overline{d\varepsilon^p} = \sqrt{\frac{2}{3}d\boldsymbol{\varepsilon}^{pT}\mathbf{C}d\boldsymbol{\varepsilon}^p} \tag{13}$$

$$\mathbf{B}=\begin{bmatrix}0 & 0 & 0\\ 0 & 1 & 0\\ 0 & 0 & 2a_{66}\end{bmatrix} \tag{14}$$

$$\mathbf{C}=\begin{bmatrix}0 & 0 & 0\\ 0 & 1 & 0\\ 0 & 0 & 1/2a_{66}\end{bmatrix} \tag{15}$$

The stress and strain components used in these definitions are taken with respect to the fiber coordinate system. The coefficient a_{66} is a material constant. The following relationship is assumed between the equivalent stress and the equivalent plastic strain:

$$\overline{\varepsilon^p}=A\left(\bar{\sigma}\right)^m \tag{16}$$

An incremental form becomes

$$\overline{d\varepsilon^p}=\frac{1}{H\left(\bar{\sigma}\right)}d\bar{\sigma} \tag{17}$$

where $H\left(\bar{\sigma}\right)$ represents an instantaneous plastic tangent modulus; i.e.

$$\frac{1}{H\left(\bar{\sigma}\right)}=Am\left(\bar{\sigma}\right)^{m-1} \tag{18}$$

Using Eq. (17), we can rewrite the plastic strain increment vector as

$$d\boldsymbol{\varepsilon}^p=\mathbf{S}^p d\boldsymbol{\varepsilon} \tag{19}$$

where

$$\mathbf{S}^p=\frac{9}{4H}\frac{1}{\bar{\sigma}^2}(\mathbf{B}\boldsymbol{\sigma})\otimes(\mathbf{B}\boldsymbol{\sigma}) \tag{20}$$

Consequently, the incremental stress-strain relation can be expressed as

$$d\boldsymbol{\sigma}=\mathbf{Q}^{ep}d\boldsymbol{\varepsilon} \tag{21}$$

where $\mathbf{Q}^{ep}(\bar{\sigma})$ represents an instantaneous elastoplastic tangent modulus; i.e.

$$\mathbf{Q}^{ep}=\left(\mathbf{S}^e+\mathbf{S}^p\right)^{-1} \tag{22}$$

and $\mathbf{S}^e$ in Eq. (22) is the reduced elastic compliance matrix.

Applying the above-described plane stress plasticity model to laminates, we can express the relationship between the stress increment in the *k*-th ply and the in-plane total strain increment of laminate as

$$d\bar{\boldsymbol{\sigma}}^{(k)}=\bar{\mathbf{Q}}^{ep(k)}d\bar{\boldsymbol{\varepsilon}}^0 \tag{23}$$

where

$$\bar{\mathbf{Q}}^{ep(k)}=\left[\bar{\mathbf{S}}^{e(k)}+\bar{\mathbf{S}}^{p(k)}\right]^{-1} \tag{24}$$

Note that the barred quantities in Eq. (24) indicate the transformed quantities in the *k*-th ply with respect to the specimen coordinate system.

The laminate constitutive model can finally be obtained as

$$d\bar{\boldsymbol{\sigma}}^0=\mathbf{A}^{ep*}d\bar{\boldsymbol{\varepsilon}}^0 \tag{25}$$

where $\mathbf{A}^{ep*}$ is the instantaneous extensional elastoplastic tangent modulus of laminates, and it is expressed as

$$\mathbf{A}^{ep*}=\frac{1}{t}\sum_k t_k\bar{\mathbf{Q}}^{ep(k)} \tag{26}$$

using the thickness of *k*-th ply t_k and the total thickness of laminate $t=\sum_k t_k$.

5. Comparison between predicted and observed results

5.1 Identification of material constants

5.1.1 Elastoplastic behavior of plies

The elastoplastic behavior of unidirectional ply is first identified. For this purpose, the constant a_{66} is determined in such a way that the off-axis stresses and strains in the form of the effective stress $\bar{\sigma}$ given by Eq. (12) and the effective plastic strain $\overline{\varepsilon^p}$ given by

$$\overline{\varepsilon^p} = \sqrt{\frac{2}{3}\boldsymbol{\varepsilon}^{pT}\mathbf{C}\boldsymbol{\varepsilon}^p} \qquad (27)$$

substantially fall on a single curve. The value of a_{66} evaluated using this procedure turned out to be $a_{66} = 1.6$, and the associated plot of $\bar{\sigma}$ against $\overline{\varepsilon^p}$ is shown in Fig. 5. Eq. (16) was fitted to the experimental effective stress-strain curve, as shown in solid line in Fig. 5, and the material constants involved were identified as $A = (1/248)^m$ MPa^{-m}, $m = 1/0.14$. The predicted off-axis stress-strain relationships of unidirectional laminate using the Sun-Chen model is shown in Fig. 6 for all the fiber orientations. We can see that good agreements have been achieved between the predicted and experimental results.

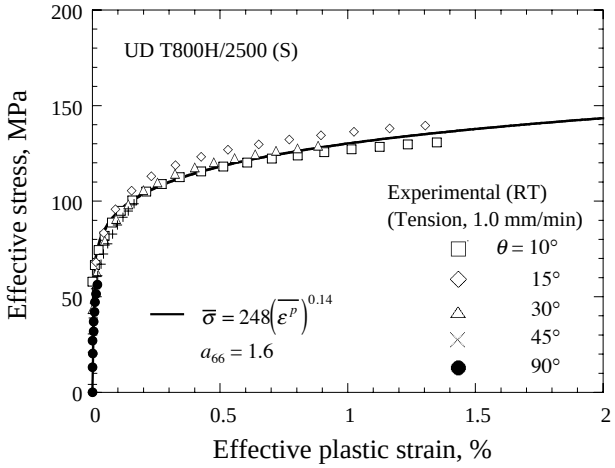

Fig. 5 Relationship between the effective stress and the effective plastic strain

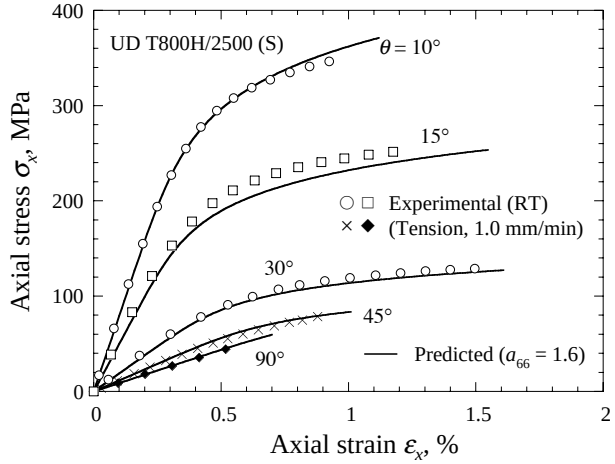

Fig. 6 Comparisons between the predicted and observed off-axis stress-stain curves for the unidirectional laminate at room temperature

5.1.2 In-situ strengths and fatigue index

As discussed in the previous study [6], the in-situ longitudinal strength X^* of unidirectional ply embedded in the alternating cross-ply laminate can be approximated by twice of the strength of the cross-ply laminate in the fiber direction. The in-situ in-plane shear strength S^* of unidirectional ply can be approximated by the shear strength calculated using the strength of the 45°-specimen of the cross-ply laminate [5]. According to the evaluation by Flaggs and Kural [2], the in-situ transverse strength Y^* comes up to about 2.48 times the transverse strength of thick unidirectional laminates. Taking into account the tendency for the in-situ strengths and an adjustment to obtain a better prediction of the fatigue behavior in the fiber direction, we finally identified the in-situ strength ratios of the embedded plies as $\alpha^* = 1.14$, $\beta^* = 2.60$, $\gamma^* = 1.30$, respectively.

Regarding the fatigue exponent for embedded thin UD plies, we assume the same value as that of isolated thick unidirectional laminates. This is because in Fig. 3 the normalized S-N relationships of the cross-ply and unidirectional laminates are in good agreement with each other, regardless of the fiber orientation. In this study, therefore, we adopted the value $n = 23.1$ [13] as the fatigue index of the fatigue life equation.

5.2 Off-axis fatigue life predictions

Predicted stress-strain relationships for the alternating cross-ply laminate using the Sun-Chen model and classical lamination theory are presented in Fig. 7 for all the fiber orientations. The fiber rotation of plies due to deformation of cross-ply laminate was taken into account to improve the accuracy of predictions. We can confirm that good agreements between the predicted and experimental stress-strain relationships have been achieved over the tested strain range.

Fatigue lives of the cross-ply laminate under off-axis loading conditions were evaluated by assuming the fatigue failure criterion in which fatigue failure of cross-ply laminate occurs at the instant of fatigue failure of critical plies sustaining a larger stress in the fiber direction. The stress components in the plies embedded in the cross-ply laminate for a given maximum fatigue load were calculated using the above-described laminate elastoplasticity model. The off-axis S-N

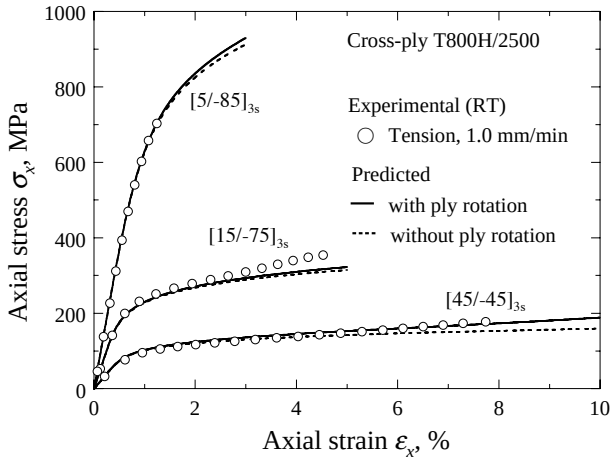

Fig. 7 Comparisons between the predicted and observed stress-strain curves for the cross-ply laminates at room temperature

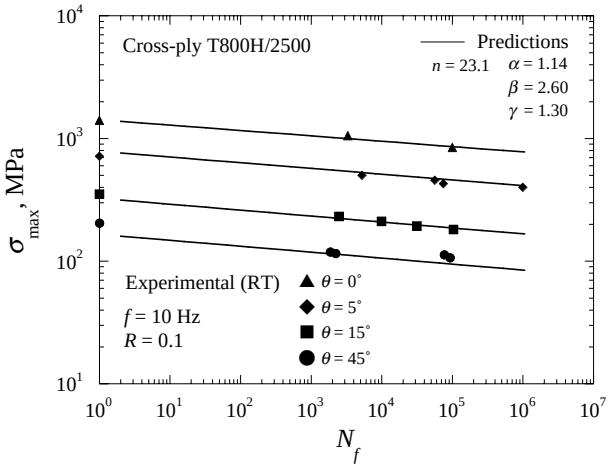

Fig. 8 On- and off-axis S-N relationships predicted from the ply-by-ply basis fatigue analysis

relationships predicted on a critical ply basis assuming the in-situ strength ratios are compared with the experimental results in Fig. 8. It is seen that the use of these in-situ strengths ratios leads to satisfactory predictions over the range of fatigue life.

Consequently, the off-axis fatigue behavior of the alternating cross-ply laminate can successfully be predicted using the ply-by-ply basis fatigue life prediction method that considers the nonlinear deformation of plies in the laminate. From additional studies on sensitivity of the in-situ shear strength ratio, it was also found that a slightly lower value of shear in-situ strength ratio compared with that evaluated on the basis of static shear strength of the laminate gave rise to better predictions.

6. Conclusions

In-situ strength based fatigue life prediction method is tested for off-axis fatigue behavior of symmetric alternating cross-ply carbon/epoxy laminate at room temperature. For this purpose, off-axis tension-tension fatigue behavior of the cross-ply laminate was first examined. Then, ply-by-ply basis fatigue life analysis of the cross-ply laminate was attempted by taking into account the in-situ static strength and off-axis nonlinear deformation of plies. Finally, validity of the proposed methodology was evaluated by comparing with experimental results. The results obtained can be summarized as follows:

(1) The off-axis S-N relationship of the cross-ply laminate can approximately be described by a straight line over the range of fatigue life up to $N_f \leq 10^6$, regardless of the fiber orientation. The straight lines fitted to those fatigue data are almost parallel with each other, and they are extrapolated back to the static strengths plotted at $N_f = 1$.

(2) The fiber orientation dependence of the off-axis S-N relationships of the cross-ply laminate can be removed by normalization with respect to static strength. The normalized S-N relationship for the cross-ply laminate agrees well with that of the unidirectional laminate.

(3) A ply fatigue model that takes into account the in-situ static strengths of plies embedded in laminates was formulated for the off-axis fatigue of a unidirectional ply. By combining the ply fatigue model with the classical lamination theory that considers the inelastic behavior of plies under off-axis loading, a general ply-by-ply basis fatigue life prediction method was also developed.

(4) The off-axis fatigue behavior of the alternating cross-ply CFRP laminate can adequately be predicted using the proposed ply-by-ply basis fatigue life prediction method.

References

[1] Sun C.T. and Jen K.C. “On the effect of matrix cracks on laminate strength”. *Proc. 1st. Conf. American Society of Composite Materials*, Dayton, OH, pp 352-367, 1987.

[2] Flaggs D.L. and Kural M.H. “Experimental determination of the in situ transverse lamina strength in graphite/epoxy laminates”. *Journal of Composite Materials*, Vol. 16, pp 103-116, 1982.

[3] O'Brien T.K. and Salpekar S.A. “Scale effects on the transverse tensile strength o graphite/epoxy composites”. In: Camponeschi ET. Jr., Editor.

Composite Materials: Testing and Design. ASTM STP 1206, ASTM, pp 23-52, 1993.

[4] Chang F.K. and Chen M.H. "The in situ ply shear strength distributions in graphite/epoxy laminated composites". *Journal of Composite Materials*, Vol. 21, pp 708-733, 1987.

[5] Yamada S.E. and Sun C.T. "Analysis of laminate strength and its distribution". *Journal of Composite Materials*, Vol. 12, pp 275-284, 1978.

[6] Rotem A., Hashin Z. "Fatigue failure of angle ply laminates". *AIAA Journal*, Vol. 14, No. 7, pp 868-872, 1976.

[7] Rotem A. "Fatigue failure of multidirectional laminates". *AIAA Journal*, Vol. 17, No. 3, pp 271-277, 1979.

[8] Lee J.W., Daniel I.M. and Yaniv G. "Fatigue life prediction of cross-ply composite laminates". In: Lagace PA, Editor. *Composite materials: fatigue and Fracture*, Second Volume, ASTM STP 1012, ASTM, pp 19-28, 1989.

[9] Gao Z. "A cumulative damage model for fatigue life of composite laminates". *Journal of Reinforced Plastics and Composites*, Vol. 13, pp 128-141, 1994.

[10] Kawai M. and Maki N. "Fatigue strengths of cross-ply CFRP laminates at room and high temperatures and its phenomenological modeling". *International Journal of Fatigue*, Vol. 28, pp 1297-1306, 2006.

[11] Kawai M. "Damage mechanics model for off-axis fatigue behavior of unidirectional carbon fiber-reinforced composites at room and high temperatures". In: Massard, T. and Vautrin, A. (eds.), *Proc. of 12th Int. Conf. on Composite Materials* (ICCM12), Paris, France, July 5-9, p 322, 1999.

[12] Kawai M. "A phenomenological model for off-axis fatigue behavior of unidirectional polymer matrix composites under different stress ratios". *Composites Part A*, Vol. 35, No. 7-8, pp 955-963, 2004.

[13] Kawai M. and Suda H. "Effects of non-negative mean stress on the off-axis fatigue behavior of unidirectional carbon/epoxy composites at room temperature". *Journal of Composite Materials*, Vol. 38, No. 10, pp 833-854, 2004.

[14] Sun C.T. and Chen J.L. "A simple flow rule for characterizing nonlinear behavior of fiber composites". *Journal of Composite Materials*, Vol. 23, pp 1009-1020, 1989.